The EMBO Journal Vol. 20 No. 9 pp. 2171–2179, 2001

cdc42 regulates the exit of apical and basolateral proteins from the *trans*-Golgi network

Anne Müsch[1,2], David Cohen, Geri Kreitzer and Enrique Rodriguez-Boulan[2,3]

Dyson Institute of Vision Research, Departments of [1]Biochemistry and [3]Cell Biology, Joan and Sanford Weill Medical College of Cornell University, New York, NY 10021, USA

[2]Corresponding authors
e-mail: amuesch@mail.med.cornell.edu or boulan@mail.med.cornell.edu

It is well established that Rho-GTPases regulate vesicle fusion and fission events at the plasma membrane through their modulatory role on the cortical actin cytoskeleton. In contrast, their effects on intracellular transport processes and actin pools are less clear. It was recently shown that cdc42 associates with the Golgi apparatus in an ARF-dependent manner, similarly to coat proteins involved in vesicle formation and to several actin-binding proteins. We report here that mutants of cdc42 inhibited the exit of basolateral proteins from the *trans*-Golgi network (TGN), while stimulating the exit of an apical marker, in two different transport assays. This regulation may result from modulation of the actin cytoskeleton, as GTPase-deficient cdc42 depleted a perinuclear actin pool that rapidly exchanges with exogenous fluorescent actin.
Keywords: cdc42/Golgi/protein transport

Introduction

It has become increasingly clear that the actin cytoskeleton participates in protein trafficking. The generation of endocytic vesicles and the docking and fusion of secretory granules with the plasma membrane require a specific reorganization of peripheral actin filaments mediated by small GTPases of the Arf (Song *et al*., 1998; Radhakrishna *et al*., 1999) and rho (for review see Ellis and Mellor, 2000) families, and involves actin-based motors (for review see X.Wu *et al*., 2000). Surprisingly, however, there is little evidence for the involvement of actin in the constitutive secretory pathway. Disruption of the actin cytoskeleton failed to affect secretion in several constitutively secreting cell lines (Griffin and Compans, 1979; Genty and Bussereau, 1980; Salas *et al*., 1986) and did not alter the kinetics of post-Golgi transport to the cell surface when only this leg of the secretory pathway was analyzed (Babia *et al*., 1999; di Campli *et al*., 1999). However, since most of these studies focused on multi-step pathways, the negative data obtained could reflect opposite roles of the actin cytoskeleton in individual steps of the pathway. Indeed, recent evidence suggests that actin could play key regulatory roles at various intracellular transport steps in the secretory pathway. The discovery of actin-binding proteins, notably spectrin, ankyrin and several myosins, at the Golgi and *trans*-Golgi network (TGN) has led to the speculation that budding and fusion events at this organelle are also regulated by an actin-based cytoskeleton (De Matteis and Morrow, 1998; Heimann *et al*., 1999; Valderrama *et al*., 2000). However, in contrast to cortical actin microfilaments, Golgi-associated actin filaments are not readily detectable when cells are probed with phalloidin, suggesting that a Golgi-based actin network might be highly dynamic.

In an attempt to characterize the nature of putative Golgi-based actin microfilaments and their role in protein transport, we searched for regulators of actin polymerization at the Golgi. cdc42, a key modulator of cortical actin at the plasma membrane, was a prime candidate since it is the only rho-GTPase with a reported localization at the Golgi apparatus (Erickson *et al*., 1996). cdc42 associates with the Golgi complex in a brefeldin A (BFA)-dependent manner characteristic of coat proteins that generate transport vesicles (Robinson and Kreis, 1992). The actin-binding proteins spectrin (Beck *et al*., 1994), ankyrin (Godi *et al*., 1998) and myosin IIA (p200) (Narula *et al*., 1992) display a similar BFA-sensitive association with the Golgi apparatus, suggesting that vesicle formation from the Golgi complex and actin filament dynamics might be regulated in a concerted manner.

A recent report (Kroschewski *et al*., 1999) has implicated cdc42 in the regulation of basolateral polarity in Mardin Darby kidney (MDCK) cells. The authors observed a reversal in the polarity of the targeting of the basolateral protein vesicular stomatitis virus (VSV) G coupled to green fluorescent protein (GFP) in cells microinjected with cDNAs of VSV G–GFP and a dominant-negative mutant of cdc42. Although the mechanism for this targeting defect is unknown, a possible role for cdc42 could be to regulate the generation of basolateral transport vesicles from the most distal compartment of the Golgi, the TGN, where sorting of apical and basolateral proteins is thought to occur.

We studied protein transport in cells expressing cdc42 mutants that are defective in nucleotide binding (cdc42N17) or hydrolysis (cdc42Q61L or cdc42V12) and established that cdc42 differentially regulates the exit of apical and basolateral proteins from the TGN in MDCK cells. Time-lapse fluorescence imaging of the apical marker neurotrophin receptor p75 fused to GFP (p75–GFP) showed a 4-fold accelerated exit from the TGN in the presence of the GTPase-deficient cdc42 mutant, and the release of p75-containing vesicles from the TGN was stimulated in semi-intact cells expressing the activated GTPase. In contrast, release of basolateral proteins from the TGN was inhibited in the biochemical assay and showed slower TGN exit kinetics in live imaging experiments. The effects of activated cdc42 (cdc42V12) on protein transport from the TGN were accompanied by

changes in the organization of the actin cytoskeleton. A highly dynamic pool of actin filaments that are concentrated in the perinuclear area was detected by the incorporation of alexa 568-tagged G-actin in permeabilized cells (Symons and Mitchison, 1991). This actin pool disappeared in the presence of cdc42V12, with a concomitant enhancement of alexa 568–actin labeling in the cortical actin network. The effect of cdc42V12 on the exit of the basolateral marker neuronal cell adhesion molecule (NCAM)–GFP from the TGN could be mimicked by the actin filament-disrupting drug latrunculin B (LatB), suggesting that the regulation of basolateral protein transport from the TGN by cdc42 involves the actin cytoskeleton.

Results

Mutant cdc42 selectively regulates the exit of apical and basolateral vesicles from the TGN

To study the role of cdc42 in protein transport from the TGN, we initially utilized a permeabilized cell vesicle budding assay that measures the cytosol-dependent release of apical and basolateral TGN-derived transport vesicles in mechanically perforated cells (Müsch *et al*., 1996; Yeaman *et al*., 1998; Supplementary figure 1, available at *The EMBO Journal* Online). Briefly, we co-expressed the apical marker p75 and the basolateral marker low density lipoprotein receptor (LDLR) in MDCK cells by adenovirus-mediated gene transfer, and labeled them with [^{35}S]sulfate as they accumulated in the TGN during a 20°C block. We separated the transport vesicles released during a 1 h incubation at 37°C in the presence of cytosol and an energy-regenerating system by sedimentation of the semi-intact cells, and quantified the amount of radiolabeled p75 and LDLR in pellet and vesicle fractions. Vesicle release was measured in MDCK cell lines expressing myc-tagged recombinant cdc42V12 (GTPase-deficient form) or cdc42N17 (nucleotide-free form) under the control of a tetracycline-regulated repressor, which allowed the induction of recombinant cdc42 proteins at levels between 0.5- and 10-fold higher than endogenous cdc42 in different clones (Figure 1A). Vesicle release was studied in three clones with different expression levels of each cdc42 mutant and compared with that in three clones derived from the parental cell line, which expresses the tetracycline-regulated repressor protein but no recombinant cdc42 molecules.

The expression of cdc42V12 caused a significant increase in cytosol-dependent vesicle release of p75 from the TGN, ~30% in all three clones, regardless of the expression level, while the release of LDLR-containing vesicles from the same cells was inhibited by ~30% in two of the three clones tested (Figure 1B). The lack of effect of cdc42V12 on LDLR release in clone 3 did not correlate with the lowest expression level for the cdc42 mutant, and is likely to represent a clonal peculiarity (compare Figure 1A and B). In contrast, the nucleotide-free mutant cdc42N17 caused an inhibition of LDLR vesicle budding in the higher-expressing clones 1 and 3, while the low-expressing clone 2 was not different from the control clones (compare Figure 1A and B). We observed no significant effect of cdc42N17 expression on the release of p75-containing vesicles.

We tested the possibility that the changes in TGN release elicited by cdc42 mutants were the consequence of effects on earlier steps in the secretory pathway that resulted in altered transport to the Golgi compartment and accumulation of cargo at 20°C. However, we found no differences in the kinetics of *O*-glycosylation (a Golgi function) of p75/LDLR in the cdc42V12- and cdc42N17-expressing cell lines (Figure 1C). Taken together with these data, the results obtained with the vesicle budding assay indicate that cdc42 regulates differentially the exit of apical and basolateral vesicles from the TGN.

The effects obtained with the *in vitro* vesicle budding assay were statistically significant but moderate. We reasoned that a regulatory role of cdc42 in TGN exit pathways would be reflected better in an assay that measures the kinetics of protein exit *in vivo*, rather than the maximal amounts of vesicles released *in vitro* from the TGN. Therefore, we studied the effect of constitutively activated cdc42 on the exit kinetics of apical and basolateral proteins from the TGN by time-lapse imaging of C-terminal GFP-tagged markers, as previously described for p75–GFP (Kreitzer *et al*., 2000). We microinjected the cDNAs of the apical marker p75–GFP, or of NCAM–GFP, a basolateral marker, into the nucleus of sub-confluent cells, and allowed their accumulation in the TGN by incubation for 1 h at 37°C followed by a 20°C block in the presence of cycloheximide. Co-expression of either activated cdc42 (cdc42Q61L) or nucleotide-free cdc42 (cdc42N17) did not interfere with the transport of the markers to the Golgi (Figure 2B) and did not cause changes in cell shape or Golgi morphology that could influence the imaging (Figure 2B and data not shown). The GFP tag attached to the C-terminus did not affect the basolateral polarity of NCAM in confluent MDCK cells (Figure 2A), or the apical polarity of p75 (Kreitzer *et al*., 2000). We used NCAM–GFP rather than LDLR as a basolateral marker in this assay, as preliminary experiments showed that internalization of LDLR after delivery to the plasma membrane interfered with the analysis of its exit from the TGN.

We quantified the exit kinetics of the GFP fusion proteins from the Golgi by measuring the redistribution of Golgi-associated GFP to peripheral regions in the cell, as described previously (Kreitzer *et al*., 2000). Co-expression of cdc42 mutants with the GFP fusion proteins dramatically accelerated the exit of p75–GFP. Constitutively activated cdc42 (cdc42Q61L) reduced the half-time of TGN emptying from ~110 to ~20 min, while expression of nucleotide-free cdc42N17 resulted in a half-time of ~40 min for the exit of p75–GFP (Figure 2C). In contrast, the exit of NCAM–GFP from the Golgi was slowed down by overexpression of cdc42Q61L and cdc42N17 (Figure 2D). The half-time of TGN emptying was increased from ~20 to ~40 min (for cdc42Q61L) and ~32 min (for cdc42N17); these changes were statistically significant ($p < 0.0001$ and < 0.01, respectively). These live imaging results, together with the data obtained with the *in vitro* vesicle budding assay, demonstrate conclusively that cdc42 differentially controls protein exit pathways emerging from the TGN. The exit of a model apical protein is enhanced, whereas the exit of basolateral proteins is slowed down by cdc42 mutants. The effect of cdc42 mutants is clearly a kinetic one that causes

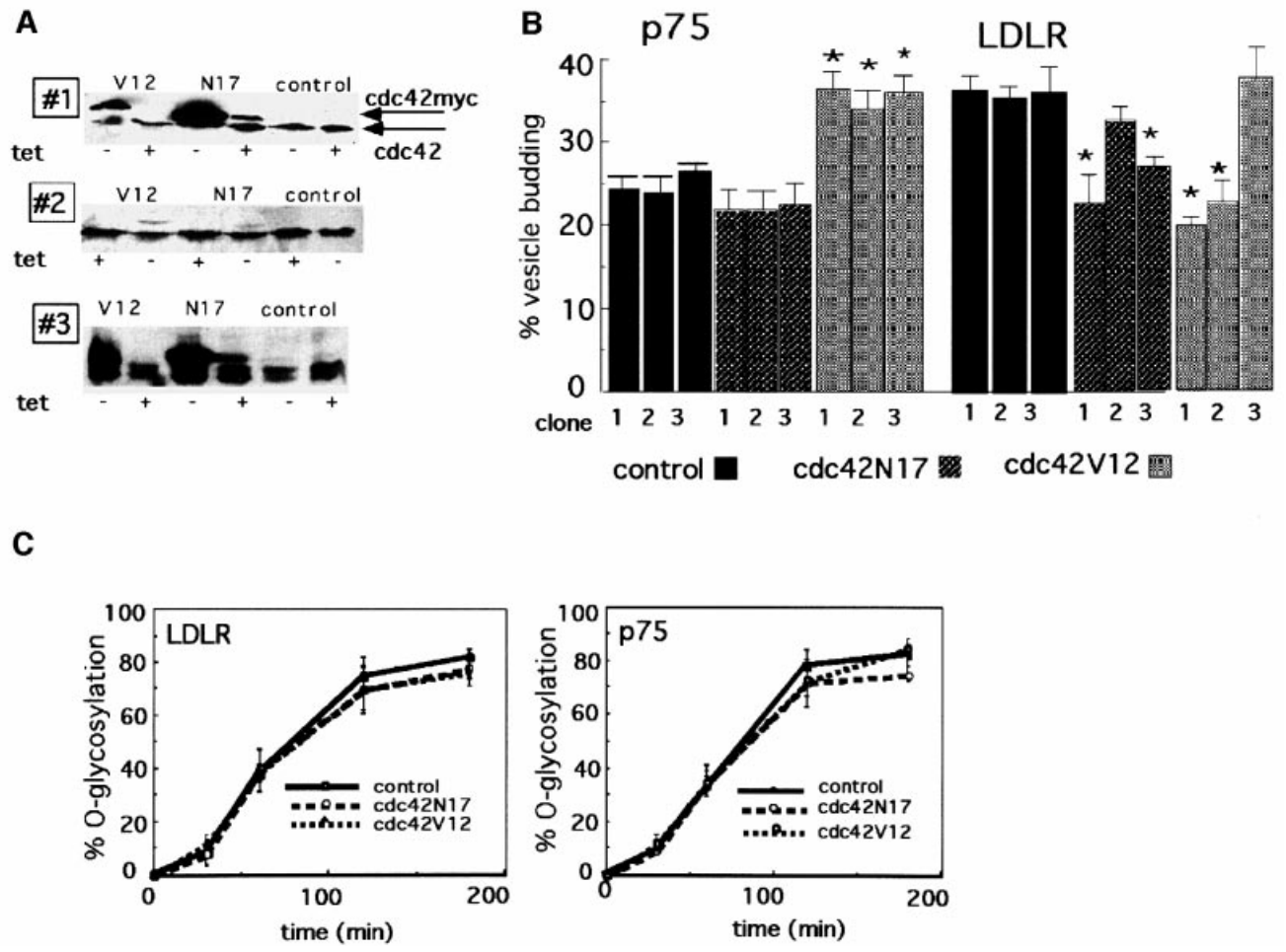

Fig. 1. The release of p75-containing vesicles from the TGN *in vitro* is stimulated in cdc42N17- and cdc42V12-expressing cells, while the release of LDLR-containing vesicles is inhibited. (**A**) Regulated expression of cdc42 mutants in MDCK cells. A western blot probed with cdc42 antibodies of cell lysates prepared from control cells and three clones of cdc42N17 and cdc42V12 grown in the presence (+tet) or absence (–tet) of doxycycline as described in Materials and methods. The less mobile band represents myc-tagged recombinant cdc42; the lower band is endogenous cdc42. (**B**) Vesicle budding from the TGN. The release of p75 (left panels) and LDLR (right panels) containing vesicles from the TGN in the presence of cytosol in semi-intact cells as described in Materials and methods. Black bars, three clones of control cells; striped bars, three clones of cdc42N17-expressing cells; gray bars, three clones of cdc42V12-expressing cells; clone numbers correspond to those in (A). The asterisk indicates a significant difference compared with each of the control clones with $p < 0.001$; data are from four experiments (for cdc42V12 and N17) and three experiments (for the control clones) with samples in triplicates. (**C**) Kinetics of p75/LDLR transport to the late Golgi. p75 and LDLR were pulse labeled with [^{35}S]cysteine for 15 min and chased for 30, 60, 120 and 180 min in the presence of excess cysteine. The *O*-glycosylated protein can be resolved from its precursor in PAGE due to its higher molecular weight. The graph depicts the percentage of *O*-glycosylated p75/LDLR of total marker. Data are from three experiments in duplicates with SE.

drastically different half-times for the exit of a population of cargo proteins from the TGN, but eventually all of the GFP-tagged proteins are released from the Golgi even in the presence of cdc42 mutants. This may explain why the changes in Golgi exit observed were considerably larger in the live imaging experiments (55% to 5-fold) than in the budding assay (~30%), which measures the 'endpoint situation' of protein exit from the TGN. That the budding assay revealed any effect of cdc42 mutants on protein exit from the TGN at all is most likely due to the fact that a kinetic disadvantage *in vivo* is translated into a diminished capacity of the semi-intact cells for protein transport *in vitro*.

The results obtained by time-lapse imaging indicate further that the activated mutant of cdc42 is more efficient than the nucleotide-free form in altering protein transport from the TGN, suggesting an explanation for why cdc42V12, but not cdc42N17, stimulated p75 vesicle budding *in vitro*.

Alexa 568–G-actin labels a perinuclear actin cytoskeleton in permeabilized cells that is regulated by cdc42

Our data suggest a selective regulatory role of cdc42 in constitutive protein transport at the level of the TGN. Since the signaling cascades of cdc42 often result in a re-organization of the cellular actin cytoskeleton, we were interested in the effects of cdc42V12 expression on the overall distribution of actin, with a particular focus on actin in the perinuclear area. Although fluorescent phalloidin labels a diffuse perinuclear actin pool (Valderrama

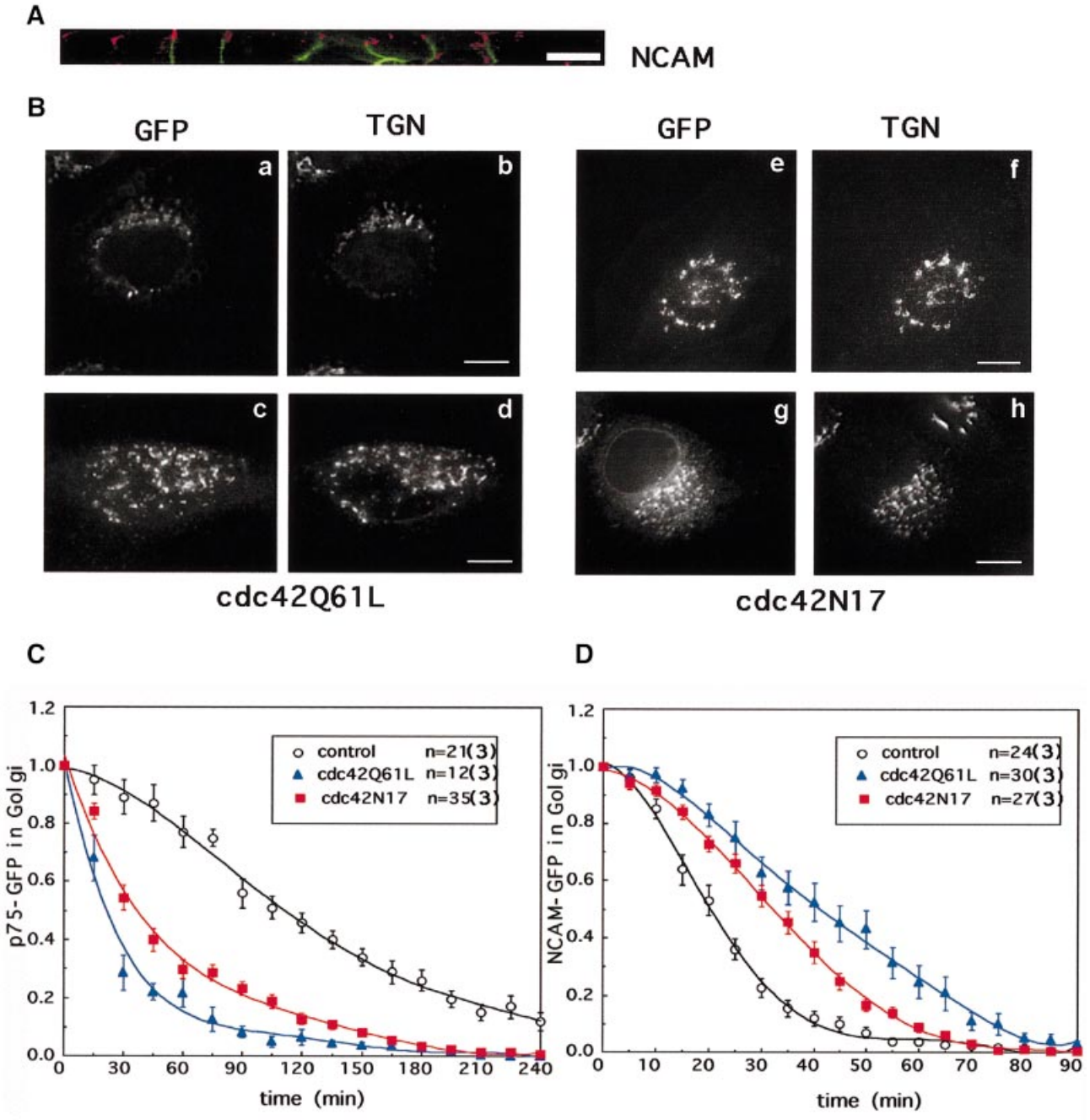

Fig. 2. The exit of p75–GFP from the TGN is accelerated in cdc42Q61L- and cdc42Y57-expressing cells, while the exit of NCAM–GFP is delayed. (**A**) Targeting of NCAM–GFP to the lateral surface in confluent MDCK cells; cells were fixed in PFA and labeled with anti-ZO-1 (red); GFP fluorescence in green; scale bar = 10 μm. (**B**) Accumulation of NCAM–GFP (a, b, e and f) and p75–GFP (c, d, g and h) in the TGN after the 20°C block in the presence of cdc42Q61L (a–d) or cdc42N17 (e–h). Cells were fixed with methanol, and GFP fluorescence (a, c, e and g) was co-localized by indirect immunofluorescence with a marker for the TGN (b, d, f and h); scale bar = 20 μm. (**C** and **D**) Exit of p75–GFP (C) or NCAM–GFP (D) from the TGN recorded in 15 min intervals over 4 h (C) or in 5 min intervals over 95 min (D). The amount of GFP fluorescence in the perinuclear area was quantified for each time point and normalized to total cell fluorescence. Data are expressed as a percentage of the Golgi fluorescence at time 0 and plotted as a function of time after the temperature shift to 33°C with SE; n = number of cells analyzed for each condition with the number of experiments in parentheses. Differences in p75–GFP exit between control and cdc42Q61L/cdc42N17-expressing cells are significant at 30 min and all subsequent time points (p <0.0001). Differences in NCAM–GFP exit between control and cdc42Q61L cells are significant at all time points between 10 and 60 min, and for cdc42N17 between 15 and 60 min (p <0.01).

et al., 1998), a putative Golgi-based actin cytoskeleton has eluded detection under the light microscope.

As transient and highly dynamic microfilaments might escape detection by standard phalloidin staining, we adapted to our system a technique that measures the incorporation of alexa 568-labeled G-actin into the barbed ends of free, elongating actin filaments at fibroblastic lamellae (Symons and Mitchison, 1991). We briefly exposed mechanically perforated MDCK cells to alexa 568-labeled actin monomers and antibodies against the cytoplasmic domain of Golgi proteins, and fixed the cells with glutaraldehyde. In control cells, alexa 568–G-actin

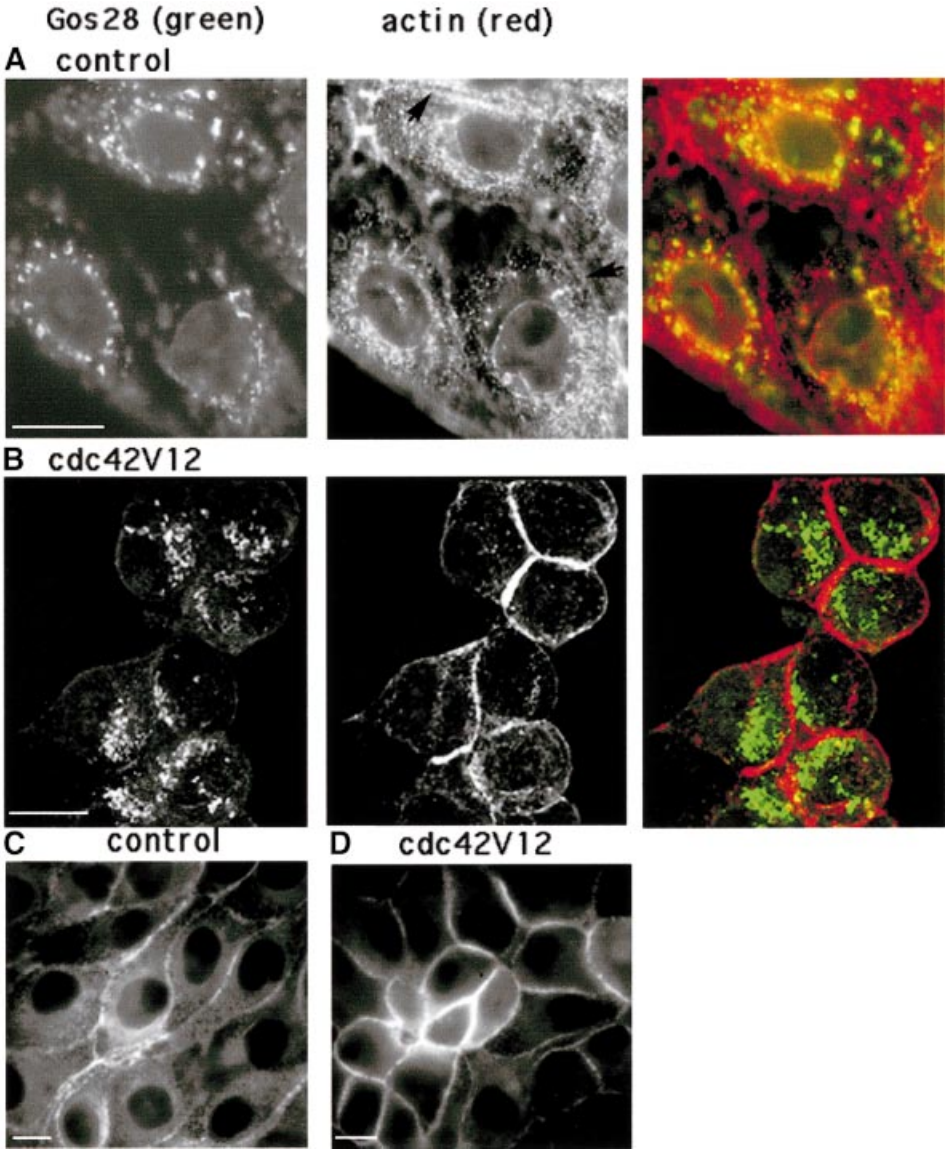

Fig. 3. Alexa 568–G-actin labels a perinuclear actin cytoskeleton in permeabilized cells that is absent in cdc42V12-expressing cells. (**A** and **B**) Mechanically permeabilized control cells (A) or cdc42V12-expressing cells (B) were incubated with alexa 568–G-actin and anti-Gos28 antibodies for 5 min and then fixed as described in Materials and methods. (A) Optical slice in the Golgi region of a series of 0.5 μm optical sections through the cell; the arrow points to actin at the cell cortex. (B) 3D reconstruction of 0.5 μm optical sections through the cell; left panel, alexa 568–actin; middle panel, Gos28; right panel, overlay with actin in red and Gos28 in green. (**C** and **D**) Control (C) or cdc42V12-expressing (D) cells were fixed with PFA after a 45 s pre-extraction with 0.1% Triton X-100 on ice and labeled with FITC–phalloidin. Scale bar = 2.5 μm.

was readily incorporated into the cortical actin cytoskeleton, but in addition, labeled short filaments in the cytoplasm, which were abundant and often appeared to originate in the perinuclear area (Figure 3A, middle panel). Many of these perinuclear actin filaments aligned closely with Golgi elements (Figure 3A, left and right panels). In contrast to control cells, neither perinuclear nor other cytoplasmic actin filaments were visible in cdc42V12-expressing cells; instead, these cells displayed an apparent enhancement of alexa 568–actin fluorescence incorporation into the cortical actin cytoskeleton (Figure 3B). Fluorescent phalloidin staining detected a decrease in perinuclear and intracellular staining in cdc42V12-expressing cells (Figure 3C and D), consistent with a depletion of perinuclear actin rather than with a selective block in the incorporation of G-actin into perinuclear filaments by cdc42. Expression of cdc42N17 did not reveal obvious differences in the distribution of alexa 568–actin to control cells. This might correlate with the more moderate effect of this cdc42 mutant on vesicle transport from the TGN. The prominent redistribution of actin to the cell cortex in cdc42V12-expressing cells occurred mainly to the basal but not the apical pole of the cell (see Figure 3B, which represents a reconstruction of all *x*–*y* planes through the cell). This is in agreement with a previous observation by Kroschewski *et al*. (1999). In contrast to these authors, however, we did not observe the flattening of the cells that they associate with the changes in the organization of cortical actin filaments, but rather a rounding of the cells (compare Figure 3A and B). This discrepancy could be due to the different expression levels of the cdc42 mutants in microinjected cells versus transfected cell lines.

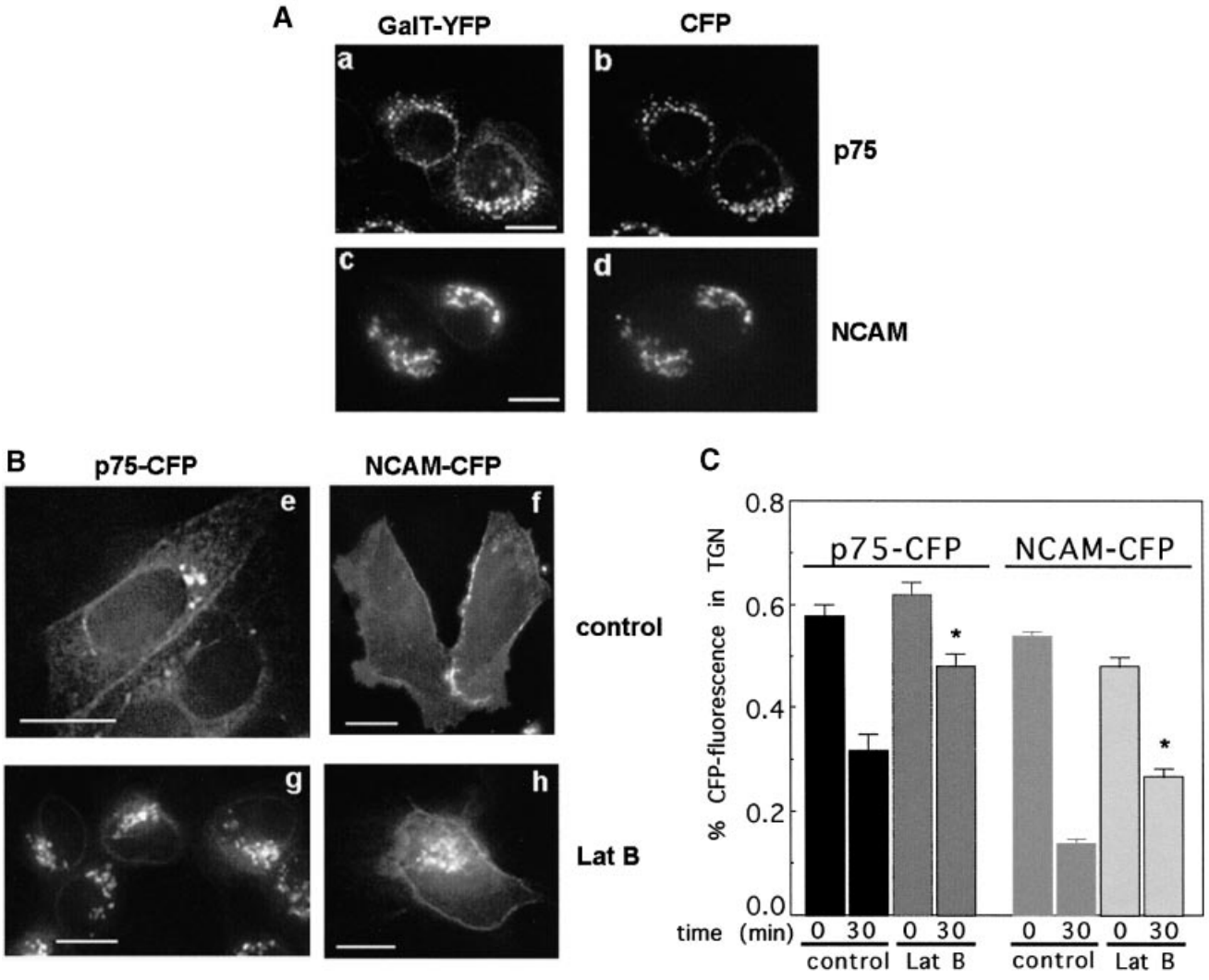

Fig. 4. LatB inhibits the exit of p75–CFP and NCAM–CFP from the TGN. (A and B) Individual optical slices from a series of 0.5 μm sections through p75–CFP- and GalT–YFP- (a, b, e and g) or NCAM–CFP- and GalT–YFP- (c, d, f and h) expressing cells. (**A**) Co-localization of GalT–YFP (a and c) with p75–CFP (b) or NCAM–CFP (d) after the 20°C block and LatB pre-treatment; scale bar = 2 μm. (**B**) p75–CFP (e and g) or NCAM–CFP (f and h) 30 min after the release from the TGN at 33°C in the absence (e and f) or presence (g and h) of LatB. (**C**) Quantitation of NCAM/p75–CFP fluorescence that co-localized with GalT fluorescence in control and Lat-treated cells at the end of the 20°C block (time 0) and after 30 min at 33°C (time 30 min). The sum of either Golgi-associated or total cell fluorescence throughout all stacks was determined as described in Materials and methods, and Golgi fluorescence was expressed as percentage of total cell fluorescence. Data are from 8–15 cells for each condition from two experiments with SE. The asterisk indicates a significant difference compared with control; $p < 0.0001$.

Disruption of actin microfilaments with LatB delays the exit of both NCAM–CFP and p75–CFP from the TGN

The selective effects of cdc42V12 on TGN exit pathways and perinuclear actin filament pools prompted us to test whether non-selective disruption of cellular actin filaments by LatB would have similar effects on TGN exit to the cdc42 mutant. Preliminary data indicated that LatB effectively depolymerized the actin cytoskeleton of MDCK cells after 15 min at 20°C (data not shown). As actin depolymerization by LatB induced rounding of the cells (Figure 4B), we carried out the analysis of protein exit from the Golgi in 0.5 μm optical sections of fixed cells and marked the position of the Golgi complex by co-expressing yellow fluorescent protein (YFP)-tagged 1,4-β-galactosyltransferase (GalT–YFP), a marker for the *trans*-Golgi and TGN (Taatjes *et al*., 1987), with cyan fluorescent protein (CFP)-tagged p75 (p75–CFP) or NCAM–CFP. GalT–YFP completely co-localized with p75–CFP and NCAM–CFP after the 20°C block (Figure 4A). When we quantified the amount of p75–CFP or NCAM–CFP remaining in the Golgi after the reversal of the 20°C block, we found that under control conditions, 40% (p75) and 75% (NCAM) of the CFP fluorescence initially overlapping with GalT–YFP had exited within 30 min (Figure 4B and C; Supplementary figure 2). LatB reduced this rate to 20% for p75–CFP and 45% for NCAM–CFP (Figure 4B and C). We did not analyze later time points since progressive membrane blebbing in LatB-treated cells made the distinction between surface and Golgi-associated CFP fluorescence difficult. Our data demonstrate that the actin cytoskeleton indeed regulates protein exit from the TGN. Non-selective disruption of the actin cytoskeleton mimicked the effect of cdc42 mutants on the exit of

basolateral proteins, suggesting an actin-dependent role for cdc42 in basolateral transport from the TGN. Similar to the effect of cdc42 mutants, complete actin filament disruption had a kinetic effect on basolateral protein exit from the Golgi, rather than blocking it completely. Thus, although actin filaments may facilitate basolateral protein transport from the Golgi, they do not appear to be absolutely essential for this transport step. Importantly, the exit kinetics of apical proteins from the TGN were inhibited by actin filament disruption and stimulated by expression of cdc42 mutants, suggesting that the modulatory effect of cdc42 is more subtle than just removing perinuclear actin filaments from the Golgi area.

Discussion

Our experiments provide strong support for a regulatory role of the rho family GTPase cdc42 in constitutive protein exit from the TGN. Several groups had previously reported the participation of cdc42 in vesicle transport events at the cell cortex (Brown *et al*., 1998; Caron and Hall, 1998; Gasman *et al*., 1999; Hong-Geller and Cerione, 2000). Here, we demonstrate that the GTPase selectively regulates the generation of different populations of transport vesicles from the TGN. Expression of cdc42 mutants in MDCK cells stimulated the exit of a GFP-tagged apical cargo protein (p75–GFP) from the TGN *in vivo*, and the release of p75-containing TGN-derived transport vesicles *in vitro.* In contrast, cdc42 mutants delayed the exit of the basolateral protein NCAM–GFP from the TGN in intact cells and reduced the amount of LDLR-containing vesicles released in the *in vitro* assay.

This regulation of 'constitutive' exocytic traffic by cdc42 may contribute to cell shape changes in developing epithelia, as observed for cdc42-mediated basolateral elongation in *Drosophila* disc epithelia (Eaton *et al*., 1995), or to increased membrane delivery during directed cell movements in wounded monolayers that involve polarization of the Golgi complex and the secretory machinery (Nobes and Hall, 1999).

Both activated and nucleotide-free forms of cdc42 had qualitatively similar effects on protein exit, although the activated mutant was more effective in eliciting changes in protein transport. Similarly, we found both cdc42 mutants reversed the basolateral polarity of LDLR without affecting the apical polarity of p75 (D.Cohen, A.Müsch and E.Rodriguez-Boulan, submitted). This implies that cycling of cdc42 between the GTP-bound, GDP-bound and nucleotide-free forms is essential for its function in protein transport and polarity. This cycling, and not just the activation of cdc42 upon GTP binding, has recently been shown to be responsible for at least some of its functions (Erickson *et al*., 1997; reviewed in Symons and Settleman, 2000).

Many known effects of cdc42 on plasma membrane processes result from re-organization of the cortical actin cytoskeleton. Strikingly, cdc42V12 induced dramatic changes in microfilament organization in the perinuclear region, where our experiments suggested a regulatory role in protein transport. By incorporation of fluorescent G-actin into perforated living cells, we selectively labeled highly dynamic actin filaments with free barbed ends, and excluded from staining the capped, more stable pool of microfilaments that would also label with phalloidin. This technique revealed a prominent perinuclear pool of actin filaments that overlapped with a marker for the Golgi apparatus. The experiments demonstrate, at the light microscope level, that the Golgi apparatus is embedded in an actin network. These data complement the recent demonstration of β/γ actin on vesicles budding from the Golgi by immunoelectron microscopy (Valderrama *et al*., 2000), and biochemical studies showing that actin binds to Golgi membranes *in vitro* (Müsch *et al*., 1997; Heimann *et al*., 1999; Fucini *et al*., 2000). In the presence of activated cdc42, the perinuclear microfilaments disappear completely while the cortical belt of actin becomes thicker. The accumulation of activated cdc42 at sites of cell–cell adhesion is consistent with earlier observations in MDCK cells (Kuroda *et al*., 1997; Kroschewski *et al*., 1999) and *Drosophila* epithelia (Eaton *et al*., 1995).

The removal of perinuclear actin and the inhibition of basolateral transport from the TGN by constitutively activated cdc42 were mimicked by an actin-disrupting drug, indicating that the regulation of basolateral transport by cdc42 is mediated by the actin cytoskeleton. These data are in agreement with a previous report that the residence time of VSV G–GFP in the Golgi during its passage through the secretory pathway was prolonged from 42 to 57 min when actin filaments were disrupted with cytochalasin B (Hirschberg *et al*., 1998). Release of apical transport vesicles from the TGN, in contrast, was inhibited by non-selective actin filament disruption but was stimulated by activated cdc42. This suggests either an actin-independent role for cdc42 in apical transport from the TGN or, alternatively, the regulation of a different actin modulatory mechanism from that employed by basolateral proteins. The concept of distinct roles for actin in the formation of different classes of vesicles from the Golgi is supported by *in vitro* studies that revealed different actin-binding proteins on different Golgi-derived transport vesicles (Heimann *et al*., 1999), by the characterization of two biochemically distinct pools of actin on isolated Golgi membranes (Fucini *et al*., 2000), and by our previous finding that myosin IIA is specifically involved in the release of basolateral but not apical transport vesicles from the TGN (Müsch *et al*., 1997).

What signaling cascades involving cdc42 could be responsible for a re-organization of actin in association with vesicle transport from the Golgi?

The association of cdc42 with the Golgi complex is ARF dependent (Erickson *et al*., 1996), and ARF has emerged as a key player for recruiting adapter and coat protein complexes to the Golgi apparatus, and for regulating the association of a scaffold of cytoskeletal elements with the Golgi that includes spectrin/ankyrin, myosin and actin (reviewed in Donaldson and Lippincott-Schwartz, 2000). cdc42 could be participating in the ARF-dependent coordination of cytoskeletal rearrangements with vesicle formation by activating phospholipid-modifying enzymes such as PLD and PI(3)K (Zheng *et al*., 1994; Han *et al*., 1998). As a regulator of COPI activity (W.J.Wu *et al*., 2000), cdc42 could indirectly affect the composition of distal compartments of the Golgi complex that receive and recycle vesicles from the more proximal stacks, where COPI is thought to mediate retrograde and anterograde

protein traffic. Alternatively to directly participating in vesicle formation at the Golgi, cdc42 could also regulate the recycling of transport factors from the cell surface to the TGN, a prerequisite for the continuity of exocytosis. Recent evidence by Kroschewski *et al*. (1999) had suggested a role for cdc42 in endosomal sorting.

Finally, it needs to be considered that the effect of cdc42 on protein exit from the TGN could be the result of diverting actin monomers away from the Golgi toward cdc42-induced structures at the plasma membrane. Under this assumption, other proteins that promote a re-organization of actin structures could regulate protein transport from the TGN, even if they do not reside in the Golgi. It will be interesting, therefore, to assess the role of other members of the rho family of GTPases in the dynamics of perinuclear actin filaments and apical and basolateral transport from the TGN.

Materials and methods

cDNA constructs

cDNA encoding chicken NCAM-180 (Edelman *et al*., 1987) was cloned into pEGFP-N1 and pEBFP vectors. cDNA encoding GALT–GFP was provided by J.White (Harvard University, Cambridge, MA) and subcloned into pEYFP-N1 (Clontech).

Cell lines, cell culture and infections

The cdc42V12- and cdc42N17-expressing cell lines were generated by T.-S.Jou and W.J.Nelson (Stanford University, Stanford, CA) from the MDCK cell line MDCK-Tet-OFF, which expresses the tetracycline repressor protein [stably transfected with the pTet-OFF plasmid (Clontech)]. The authors generously made these cell lines available to us before publication. The parental MDCK cell line MDCK-Tet-OFF was provided by K.Mostov (University of California, San Francisco, CA). Three clones from this cell line were generated by transfection with a plasmid providing hygromycin resistance (equivalent to a mock transfection) and served as controls for all experiments with the cdc42V12- and cdc42N17-expressing clones.

MDCK Tet-OFF cell lines were passaged in Dulbecco's modified Eagle's medium (DMEM) with 10% fetal calf serum (FCS) and 20 ng/ml doxycycline. For expression of the recombinant cdc42 mutants, cells were plated at confluency on polycarbonate filters in the absence of doxycycline for 48 h.

Infection with the recombinant adenoviruses that express human NTRp75 (generated by M.Chao, New York University, NY) and human LDLR (generated by J.Wilson) has been described in Yeaman *et al*. (1998). The propagation of the adenoviruses in 293 fibroblasts was performed as described in Falck-Pedersen (1998).

For microinjection experiments, MDCK cells were grown on coverslips as described in Kreitzer *et al*. (2000).

Immunolabeling techniques and alexa 568–actin labeling

For indirect immunofluorescence experiments, cells were fixed with 2% freshly prepared paraformaldehyde (PFA) in phosphate-buffered saline (PBS) for 15 min. The following primary antibodies were used for immunofluorescence or western blotting: a polyclonal antibody against hcdc42 (Santa Cruz); an antibody against the myc epitope (monoclonal CE9; Calbiochem); a polyclonal antibody against the Golgi SNARE Gos28 (provided by T.Soellner, Sloan Kettering Hospital, New York); a monoclonal antibody against ZO-1 (Chemicon); a monoclonal anti-chicken NCAM antibody (clone 5e; Developmental Studies Hybridoma Bank).

For labeling of permeabilized MDCK cells with G-actin–alexa Fluor568 conjugate from rabbit muscle (Molecular Probes, Eugene, OR) we followed the protocol described by Symons and Mitchison (1991) with the following modifications: cells were grown on coverslips precoated with Alcian Blue (Aldrich) and the apical membrane was removed by gently pressing a nitrocellulose filter on top of the cells and lifting it up (Simons and Virta, 1987). After the mechanical perforation, cells were immediately incubated with G-actin and anti-Gos28 antibody for 5 min before fixation.

For labeling with fluorescein isothiocyanate (FITC)–phalloidin, cells were pre-extracted in buffer A (138 mM KCl, 3 mM $MgCl_2$, 2 mM EGTA, 0.32 M sucrose, 10 mM MES pH 6.1) with 0.1% Triton X-100 for 45 s on ice before fixation with 4% PFA in buffer A.

Images were acquired on a Nikon E-600 microscope equipped with a back-illuminated cooled CCD camera (CCD 1000-PB; Roper Scientific) and a *z*-axis stepper motor (Prior) for serial sectioning. Images were transferred to a computer workstation running MetaMorph imaging software (Universal Imaging Corp.) for processing and quantitative measurements.

Live imaging and quantitation of fluorescence

Expression, accumulation in the TGN, time-lapse imaging and analysis of TGN exit rates for GFP-tagged markers were performed as described in Kreitzer *et al*. (2000) (Supplementary figures). All cDNAs were diluted to 10 μg/ml in HKCl injection buffer (10 mM HEPES, 140 mM KCl pH 7.4) prior to intranuclear microinjection. The cdc42Q61L construct is triple HA-tagged and was provided by J.Erickson and R.Cerione (Cornell University, Ithaca, NY). The cdc42N17 construct is myc-tagged and was provided by M.Symons (Picower Institute for Medical Research, Manhasset, NY). Expression of p75–GFP and NCAM–GFP always coincided with the expression of the cdc42 construct when cDNAs were co-injected, as determined by indirect immunofluorescence with an HA antibody (clone 12CA5; Boehringer) or myc (clone 9E10; Santa Cruz).

Actin depolymerization by LatB (Figure 4) induced morphological changes in overall cell shape, which prevented measurements of total fluorescence in a single focal plane. Thus, we co-expressed a late Golgi/TGN marker, GalT–YFP, with the CFP-tagged secretory proteins to ensure accurate definition of Golgi and TGN fluorescence, and modified the quantitative method: fixed cells were optically sectioned along the *z*-axis at 0.5 μm intervals using a 60× lens (plan apochromat, 1.4 NA) and CFP and YFP filter cubes (Chroma). No bleed-through from the yellow into the cyan channel was detected. Image stacks were either analyzed without processing or subjected to 3D blind deconvolution using Autodeblur (AutoQuant, Watervliet, NY) to remove out-of-focus fluorescence while maintaining relative fluorescence intensities (Wang, 1998). Both methods gave comparable results. The total Golgi CFP fluorescence of all planes that co-localized with the GalT–YFP fluorescence was measured and expressed as a percentage of the total cell CFP fluorescence in all planes.

Vesicle budding assay in semi-intact cells, in vivo transport assays

The vesicle budding assay from the TGN in semi-intact cells was performed as described in Müsch *et al*. (1996) with the following modifications: cells were grown on polycarbonate filters instead of plastic dishes. The labeling of p75 and LDLR occurred with carrier-free [^{35}S]sulfate (1 mCi/ml; NEN) in sulfate-free medium during the accumulation of the markers in the TGN at 20°C (Yeaman *et al*., 1998). Immunoprecipitation of p75 and LDLR was performed with the antibodies against the cytoplasmic domain of LDLR (clone 4A4; hybridoma from the ATCC Hybridoma bank) and with antibodies against the ectodomain of p75 (clone ME 20.4; hybridoma provided by M.Chao, New York University).

PAGE gels were exposed on PhosphorImager screens and the radioactivity quantified with the IQMac-program of Molecular Dynamics.

Statistical analysis

The significance of differences in the mean between samples was determined by two-paired *t*-test analysis. All samples were normally distributed with a normality coefficient calculated by Shapiro–Wilk of at least 0.9.

The exit rates of GFP-tagged proteins from the Golgi in Figure 2C and D were fitted by polynomial regression with R^2 values >0.995, and the t_{50} was calculated from the fitted curves.

Analysis was carried out with the Software Analyse-it for Microsoft Excel, Leeds, UK (see http://www.analyse-it.com/).

Supplementary data

Supplementary data for this paper are available at *The EMBO Journal* Online.

Acknowledgements

We are greatly indebted to Tzuu-Shuh Jou and James W.Nelson (Stanford University, Stanford, CA) who made their cdc42-expressing MDCK cell lines available to us before publication. We also thank J.Erickson and

R.Cerione (Cornell University, Ithaca, NY), J.White (Harvard University, Cambridge, MA), J.Bruces, T.Soellner (Memorial Sloan Kettering, New York, NY) and M.Symons (Picower Institute for Medical Research, Manhasset, NY) for reagents. Thanks to R.C.Wang (Cornell University, Medical College) for subcloning GalT–GFP cDNAs and to P.Brennwald and T.Ryan (Cornell University, Medical College) for critically reading the manuscript. This work was supported in part by a grant from the NIH, a Jules and Doris Stein Professorship of the Research to Prevent Blindness Foundation to E.R.-B. and an NIH NRSA fellowship to G.K.

References

Babia,T. *et al.* (1999) N-Ras induces alterations in Golgi complex architecture and in constitutive protein transport. *J. Cell Sci.*, **112**, 477–489.

Beck,K.A., Buchanan,J.A., Malhotra,V. and Nelson,W.J. (1994) Golgi spectrin: identification of an erythroid β-spectrin homolog associated with the Golgi complex. *J. Cell Biol.*, **127**, 707–723.

Brown,A.M., O'Sullivan,A.J. and Gomperts,B.D. (1998) Induction of exocytosis from permeabilized mast cells by the guanosine triphosphatases Rac and Cdc42. *Mol. Biol. Cell*, **9**, 1053–1063.

Caron,E. and Hall,A. (1998) Identification of two distinct mechanisms of phagocytosis controlled by different Rho GTPases. *Science*, **282**, 1717–1721.

De Matteis,M.A. and Morrow,J.S. (1998) The role of ankyrin and spectrin in membrane transport and domain formation. *Curr. Opin. Cell Biol.*, **10**, 542–549.

di Campli,A., Valderrama,F., Babia,T., De Matteis,M.A., Luini,A. and Egea,G. (1999) Morphological changes in the Golgi complex correlate with actin cytoskeleton rearrangements. *Cell Motil. Cytoskeleton*, **43**, 334–348.

Donaldson,J.G. and Lippincott-Schwartz,J. (2000) Sorting and signaling at the Golgi complex. *Cell*, **101**, 693–696.

Eaton,S., Auvinen,P., Luo,L., Jan,Y.N. and Simons,K. (1995) CDC42 and Rac1 control different actin-dependent processes in the *Drosophila* wing disc epithelium. *J. Cell Biol.*, **131**, 151–164.

Edelman,G.M., Murray,B.A., Mege,R.-M., Cunningham,B.A. and Gallin,W.J. (1987) Cellular expression of liver and neural cell adhesion molecules after transfection with their cDNAs results in specific cell–cell binding. *Proc. Natl Acad. Sci. USA*, **84**, 8502–8506.

Ellis,S. and Mellor,H. (2000) Regulation of endocytic traffic by rho family GTPases. *Trends Cell Biol.*, **10**, 85–88.

Erickson,J., Zhang,C., Kahn,R., Evans,T. and Cerione,R. (1996) Mammalian CDC42 is a brefeldin A-sensitive component of the Golgi apparatus. *J. Biol. Chem.*, **271**, 26850–26854.

Erickson,J., Cerione,R. and Hart,M. (1997) Identification of an actin cytoskeletal complex that includes IQGAP and the Cdc42 GTPase. *J. Biol. Chem.*, **272**, 24443–24447.

Falck-Pedersen,E. (1998) Use and application of adenovirus expression vectors. In Spector,D. (ed.), *Cells—A Laboratory Manual*, *Vol. 2: Light Microscopy of Cell Structure*. Cold Spring Harbor Laboratory Press, Cold Spring Harbor, NY, pp. 1–28.

Fucini,R.V., Navarrete,A., Vadakkan,C., Lacomis,L., Erdjument-Bromage,H., Tempst,P. and Stamnes,M. (2000) Activated ADP-ribosylation factor assembles distinct pools of actin on Golgi membranes. *J. Biol. Chem.*, **275**, 18824–18829.

Gasman,S., Chasserot-Golaz,S., Popoff,M.R., Aunis,D. and Bader,M.F. (1999) Involvement of Rho GTPases in calcium-regulated exocytosis from adrenal chromaffin cells. *J. Cell Sci.*, **112**, 4763–4771.

Genty,N. and Bussereau,F. (1980) Is cytoskeleton involved in vesicular stomatitis virus reproduction? *J. Virol.*, **34**, 777–781.

Godi,A. *et al.* (1998) ADP ribosylation factor regulates spectrin binding to the Golgi complex. *Proc. Natl Acad. Sci. USA*, **95**, 8607–8612.

Griffin,J.A. and Compans,R.W. (1979) Effect of cytochalasin B on the maturation of enveloped viruses. *J. Exp. Med.*, **150**, 379–391.

Han,J.S., Kim,H.C., Chung,J.K., Kang,H.S., Donaldson,J. and Koh,J.K. (1998) The potential role for cdc42 protein from rat brain cytosol in phospholipase D activation. *Biochem. Mol. Biol. Int.*, **45**, 1089–1103.

Heimann,K., Percival,J.M., Weinberger,R., Gunning,P. and Stow,J.L. (1999) Specific isoforms of actin-binding proteins on distinct populations of Golgi-derived vesicles. *J. Biol. Chem.*, **274**, 10743–10750.

Hirschberg,K., Miller,C.M., Ellenberg,J., Presley,J.F., Siggia,E.D., Phair,R.D. and Lippincott-Schwartz,J. (1998) Kinetic analysis of secretory protein traffic and characterization of Golgi to plasma membrane transport intermediates in living cells. *J. Cell Biol.*, **143**, 1485–1503.

Hong-Geller,E. and Cerione,R.A. (2000) Cdc42 and Rac stimulate exocytosis of secretory granules by activating the IP_3/calcium pathway in RBL-2H3 mast cells. *J. Cell Biol.*, **148**, 481–494.

Kreitzer,G., Marmorstein,A., Okamoto,P., Vallee,R. and Rodriguez-Boulan,E. (2000) Kinesin and dynamin are required for post-Golgi transport of a plasma-membrane protein. *Nature Cell Biol.*, **2**, 125–127.

Kroschewski,R., Hall,A. and Mellman,I. (1999) Cdc42 controls secretory and endocytic transport to the basolateral plasma membrane of MDCK cells. *Nature Cell Biol.*, **1**, 8–13.

Kuroda,S., Fukata,M., Fujii,K., Nakamura,T., Izawa,I. and Kaibuchi,K. (1997) Regulation of cell–cell adhesion of MDCK cells by Cdc42 and Rac1 small GTPases. *Biochem. Biophys. Res. Commun.*, **240**, 430–435.

Müsch,A., Xu,H., Shields,D. and Rodriguez-Boulan,E. (1996) Transport of vesicular stomatitis virus G protein to the cell surface is signal mediated in polarized and nonpolarized cells. *J. Cell Biol.*, **133**, 543–558.

Müsch,A., Cohen,D. and Rodriguez-Boulan,E. (1997) Myosin II is involved in the production of constitutive transport vesicles from the *trans*-Golgi network. *J. Cell Biol.*, **138**, 291–306.

Narula,N., McMorrow,I., Plopper,G., Doherty,J., Matlin,K.S., Burke,B. and Stow,J.L. (1992) Identification of a 200-kD, brefeldin-sensitive protein on Golgi membranes. *J. Cell Biol.*, **117**, 27–38.

Nobes,C.D. and Hall,A. (1999) Rho GTPases control polarity, protrusion and adhesion during cell movement. *J. Cell Biol.*, **144**, 1235–1244.

Radhakrishna,H., Al-Awar,O., Khachikian,Z. and Donaldson,J.G. (1999) ARF6 requirement for Rac ruffling suggests a role for membrane trafficking in cortical actin rearrangements. *J. Cell Sci.*, **112**, 855–866.

Robinson,M.S. and Kreis,T.E. (1992) Recruitment of coat proteins onto Golgi membranes in intact and permeabilized cells: effects of brefeldin A and G protein activators. *Cell*, **69**, 129–138.

Salas,P.J., Misek,D.E., Vega-Salas,D.E., Gundersen,D., Cereijido,M. and Rodriguez-Boulan,E. (1986) Microtubules and actin filaments are not critically involved in the biogenesis of epithelial cell surface polarity. *J. Cell Biol.*, **102**, 1853–1867.

Simons,K. and Virta,H. (1987) Perforated MDCK cells support intracellular transport. *EMBO J.*, **6**, 2241–2247.

Song,J., Khachikian,Z., Radhakrishna,H. and Donaldson,J.G. (1998) Localization of endogenous ARF6 to sites of cortical actin rearrangement and involvement of ARF6 in cell spreading. *J. Cell Sci.*, **111**, 2257–2267.

Symons,M.H. and Mitchison,T.J. (1991) Control of actin polymerization in live and permeabilized fibroblasts. *J. Cell Biol.*, **114**, 503–513.

Symons,M. and Settleman,J. (2000) Rho family GTPases: more than simple switches. *Trends Cell Biol.*, **10**, 415–419.

Taatjes,D.J., Roth,J., Weinstein,J., Paulson,J.C., Shaper,N.L. and Shaper, J.H. (1987) Codistribution of galactosyl- and sialyltransferase: reorganization of *trans* Golgi apparatus elements in hepatocytes in intact liver and cell culture. *Eur. J. Cell Biol.*, **44**, 187–194.

Valderrama,F., Babia,T., Ayala,I., Kok,J.W., Renau-Piqueras,J. and Egea,G. (1998) Actin microfilaments are essential for the cytological positioning and morphology of the Golgi complex. *Eur. J. Cell Biol.*, **76**, 9–17.

Valderrama,F., Luna,A., Babia,T., Martinez-Menarguez,J.A., Ballesta,J., Barth,H., Chaponnier,C., Renau-Piqueras,J. and Egea,G. (2000) The Golgi-associated COPI-coated buds and vesicles contain β/γ-actin. *Proc. Natl Acad. Sci. USA*, **97**, 1560–1565.

Wang,Y. (1998) Digital deconvolution of fluorescence images for biologists. *Methods Cell Biol.*, **56**, 305–315.

Wu,W.J., Erickson,J.W., Lin,R. and Cerione,R.A. (2000) The γ-subunit of the coatomer complex binds Cdc42 to mediate transformation. *Nature*, **405**, 800–804.

Wu,X., Jung,G. and Hammer,J.A.,III (2000) Functions of unconventional myosins. *Curr. Opin. Cell Biol.*, **12**, 42–51.

Yeaman,C., Burdick,D., Muesch,A. and Rodriguez-Boulan,E. (1998) Studying protein sorting and transport vesicle assembly from the *trans*-Golgi network in intact and semi-intact epithelial and neuronal cells following RNA viral infection or adenovirus-mediated gene transfer. In Celis,J.E. (ed.), *Cell Biology: A Laboratory Handbook*. Vol. 2. Academic Press, San Diego, CA, pp. 237–245.

Zheng,Y., Bagrodia,S. and Cerione,R.A. (1994) Activation of phosphoinositide 3-kinase activity by Cdc42Hs binding to p85. *J. Biol. Chem.*, **269**, 18727–18730.

Received December 11, 2000; revised March 9, 2001; accepted March 14, 2001